

Liquid Crystal Stepwise Electropolymerization

– An Approach to Create Insect Photonic Structure

Hiromasa Goto*

Division of Materials Science, Faculty of Pure and Applied Sciences, University of
Tsukuba, Tsukuba, Ibaraki, 305-8573 Japan.

E-mail: gotoh@ims.tsukuba.ac.jp; Fax: +81-298-53-4490; Tel: +81-298-53-5128



Liquid Crystal Stepwise Electropolymerization – An Approach to Create Insect Photonic Structure

A stepwise polymerization enables production of triple-layer films consisting of [cholesteric LC order]-[nematic LC order]-[cholesteric LC order] films similar to exoskeleton of insect photonic structure.

Abstract

Production of optically active or inactive laminate structures with particular morphology can provide new functional optical materials. In this study, a stepwise polymerization enables production of triple-layer films consisting of [cholesteric LC order]-[nematic LC order]-[cholesteric LC order]. This method realizes preparation of laminate structure from one kind polymer with differing molecular orientations in each layer. The optical properties of the multi-layer thin films were examined with optical absorption spectroscopy, circular dichroism, and optical rotatory dispersion measurements. The polymer shows electrochemically driven change in optical activity.

Thin polymer films consisting of the three layers (cholesteric-nematic-cholesteric orders) show turquoise blue as a structural color. The color can be tuned by electrochemical redox process based on an electrochemical doping mechanism for π -conjugated polymers. This result demonstrates that the multi-layer organic semi-conducting polymer with liquid crystal order shows structural color with multi-layer interference mechanism.

Introduction

π -Conjugated polymers have been paid attention as promising organic electronic materials. Recently, new synthesis methods for production of functional conjugated polymers, carbon nanotube/polyaniline composite films,¹ single-wall carbon nanotubes–polythiophene hybrids,² copolymers as a n-type materials,³ template polymerization with a block copolymer,⁴ nanocoatings,⁵ and polyaniline on stainless steel,⁶ have been developed.

Multi-layered π -conjugated polymer films have been developed for high-performance actuators,⁷ polyelectrolyte multi-layers,⁸ multi-layer film electrodes,⁹ laminate devices,¹⁰ nanometric multi-layered films,¹¹ multi-layer polymer stacking,¹² and layer-by-layer electrodeposition.¹³ The fabrication of multi-layered structure further expands useful possibilities by providing new functionality for polymer materials. However, preparation of multi-layer structure from one kind of material with differing molecular orientations in each layer has yet to be synthesized.

Certain types of living organisms, such as bees, Morpho butterflies,¹⁴ and birds,¹⁵ show rainbow colors in reflected light. For example, the mountain butterfly (*Papilio ulysses*) with brilliant blue color derived from photonic structure. External skeletons of golden beetles have laminated structure, constructed from multiple layers with liquid crystal (LC) ordering.¹⁶ Specifically, such photonic insects employ cholesteric LC order to form laminated structures in the cuticle. The laminated structure may be grown by using a temperature-induced phase transition of liquid crystal in the growth process of the exoskeleton. For example, the proteins of exoskeleton are produced at night in the LC temperature range to yield a cuticle layer with LC order, while the exoskeleton grown under sunlight consists of a cuticle layer that does not possess LC order in the isotropic temperature range.¹⁷ This repeated daytime/nighttime process may provide multi-layers consisting of repeated [cholesteric LC order]–[non LC order] structures.

Generally, LC materials consist of rigid rod-like molecules. These molecules form mesophase (LC phase) with the order due to the rod-like structure and the disorder due to the flexible chain in the mesogenic structure. LCs can be considered as crystals with

fluidity. However, the order of liquid crystals is not completely rigid as in true crystals. External force can deform LCs easily. However the LC order is restored after release of the external force. In other words, LCs can be tolerant to temporary external force with the capacity to restore previous order. Liquid crystals display certain optical textures under observation of polarized optical microscopy (POM). The specific optical structure depends on LC phase (eg., nematic LC shows Schlieren texture and thread-like texture; cholesteric LC exhibits fingerprint texture and Grandjean texture) without regard to molecular version. LC phases can be maintained even after addition of small amounts of non-LC molecules as contaminations. This property allows application of LCs as chemical reaction solvents.

In previous studies, we have developed an electrochemical method based on cholesteric LC to prepare optically active polymer films from non-optically active monomers.¹⁸ This method allows preparation of chiroptically active thin films with cholesteric LC order. In the present study, electrochemical polymerization in LC is performed for the preparation of semiconducting polymer films with the lamellar structure of LC order.

Nematic is an achiral LC phase. The directors (local direction of LC molecules) of nematic LC orient along one direction. Cholesteric LC is a chiral LC phase in which the director (temporal and spatial average of the long molecular axis) is continuously twisted about a helical axis oriented perpendicular to the long axis of the molecule. Directors of cholesteric LC form helical structure. Cholesteric LC has chirality derived from three-dimensional helical structure. Nematic phase (non-chiral LC) is transformed into cholesteric LC with addition of a small amount of chiral compounds (referred to as chiral dopants or chiral inducers). Therefore, there are two methods for the preparation of cholesteric LC: 1) synthesis of chiral LC; and 2) the addition of a chiral inducer to nematic LC.

In this research, cholesterol pelargonate (Ch*-PEL, Table 1) is employed as a chiral inducer to *n*-hexyl-cyanobiphenyl (6CB, nematic LC solution), and the resultant cholesteric LC solution and the nematic LC solution (6CB) are used for the polymerization solution.

Electrochemical polymerization is a convenient method for preparation of π -conjugated polymers. Generally, electrochemical polymerization is carried out in electrolyte solution containing monomer with application of voltage. The resultant polymer adheres to the electrode. The polymer thus obtained with the electrochemical method shows electrochromism (color change with redox cycle in electrolyte solution).

Stepwise polymerizations in LC, developed in this study, are carried out to obtain

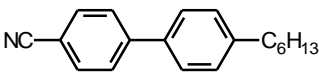
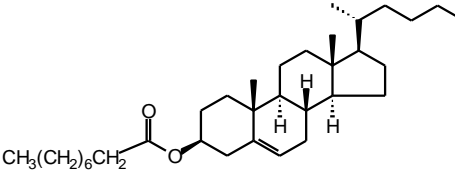
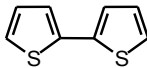
laminated structure of a π -conjugated polymer showing structural color.

Cholesteric LC has been employed for coating materials showing rainbow color. It shows selective reflection of light in the Grandjean orientation (planar orientation with the helical axis perpendicular to the substrate). In the case of cholesteric LC with Grandjean texture, the film shows selective reflection of light. But homeotropic orientation (the helical axis parallel to substrate) affords diffraction derived from periodic fingerprint patterns. In other words, cholesteric LC with fingerprint texture and Grandjean texture function as diffraction gratings and selective reflectors.

The selective reflection and diffraction from cholesteric LC show interference rainbow color upon irradiation by white light. The Morpho butterfly combines both selective reflection and diffraction functions. Many insects use multi-layer systems, although an insect employing gratings to show iridescence has been reported.^{16(a)} So far, a combination of grating and multilayer systems showing structural color with LC order has not been found to date.

The effort in this research is directed to preparation of a new type of photonic film having both grating and selective reflection of light functions with a three-layer LC ordered polymer to approach realization of artificial morho-butterflies having both multilayer reflection and grating functions.

Table 1. Molecular structures of compounds in liquid crystal electrolyte solutions.

Materials	Function	Molecular structure
<i>n</i> -Hexyl-cyanobiphenyl (6CB)	Matrix LC	
Cholesteryl pelargonate (Ch*-PEL)	Ch*-inducer	
Tetra <i>n</i> -butyl ammonium perchlorate TBAP (TBAP)	Supporting electrolyte	$N^+(C_4H_9)ClO_4^-$
Bithiophene (BT)	Monomer	

Experiment

General procedure of electrochemical polymerization in liquid crystals

Electrochemical polymerization is an effective method of preparing π -conjugated polymers. The electroactive polymers have been studied for application in electrochromic devices with transparent electrodes.¹⁹⁻²¹

Electrochemical polymerization in the LC electrolyte solution creates a polymer with LC order, with a characteristic Schlieren texture and fingerprint structure, very similar to that of liquid crystals.²² In this study, electrochemical polymerization of the monomers in LC electrolyte solution was sequentially carried out for obtaining a multi-layer structure.

The present electrochemical polymerization was carried out with the sandwich-cell LC polymerization method that the author has developed. Prior to electrochemical polymerization, the LC electrolyte solution was heated in a vial under argon atmosphere in order to completely dissolve the contents of the electrolyte solution, such as the supporting electrolyte, the monomer, and the chiral inducer (in the case of preparation of cholesteric LC), in 4-*n*-hexyl-4'-cyanobiphenyl (6CB). The LC electrolyte was injected by using the capillary technique between two sandwiched indium-tin-oxide (ITO) coated glass electrodes with a Teflon sheet (thickness = 0.2 mm) used as a spacer. The reaction cell was initially heated under argon atmosphere to ca. 60 °C, and then gradually cooled to room temperature. Then, a constant 4.0 V was applied across the cell. After the polymerization, an insoluble and infusible polymeric thin film was obtained at the anode side of the ITO electrode. The film on the ITO was then washed with acetone and tetrahydrofuran (THF) in that order. Subsequently, another polymerization on the film was carried out using the same procedure for the preparation of a multi-layer polymer film. Fig. 1 shows differential scanning calorimetry (DSC) results for the LC electrolyte solution containing monomers. Transition temperatures of the nematic LC solution containing monomer and supporting electrolyte and cholesteric LC electrolyte solution containing monomer, supporting electrolyte, and the chiral inducer are Cr·13.5(-4.1)·N·23(21)·Iso and Cr*·11(-5<)·Ch*·19(18)·Iso*, respectively (Cr = crystal, N = nematic, Iso = isotropic, * indicates chiral).

Note that polymers thus obtained show clear fingerprint texture. The optical structure is very similar to that of the LC electrolyte solution used for the electrochemical polymerization. Molecular structures of the compounds employed in this study are summarized in Table 1.

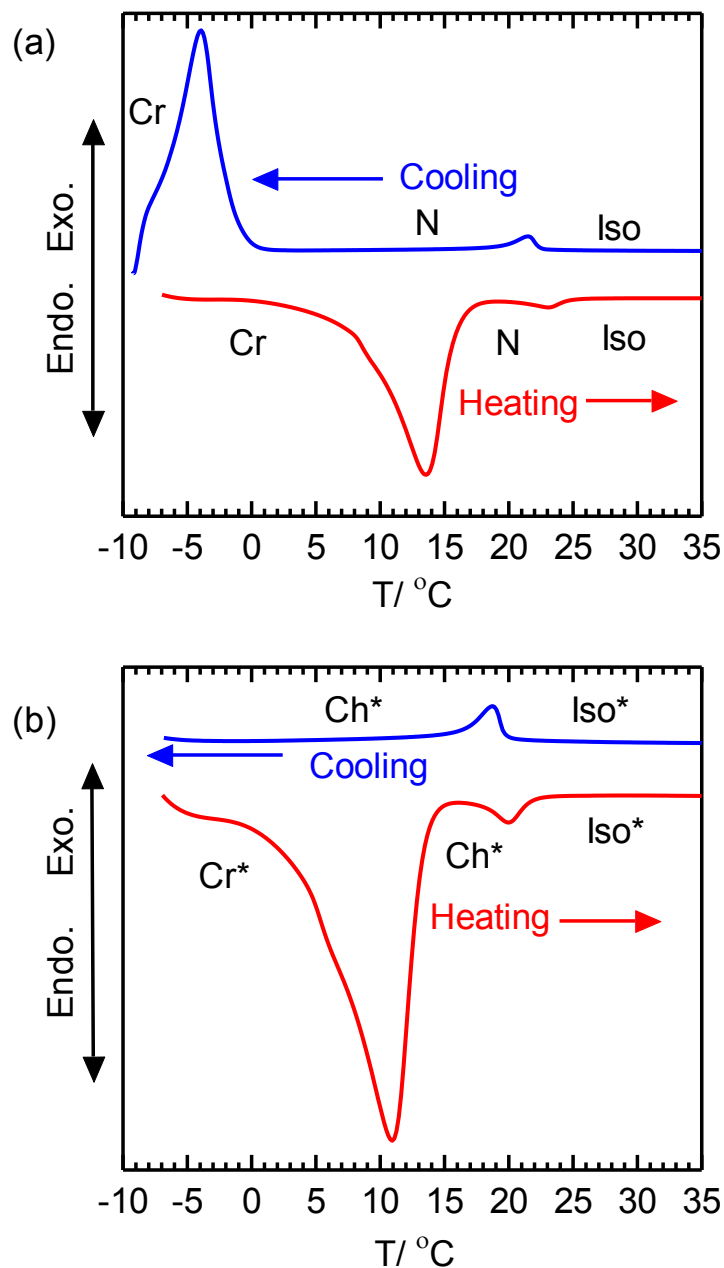


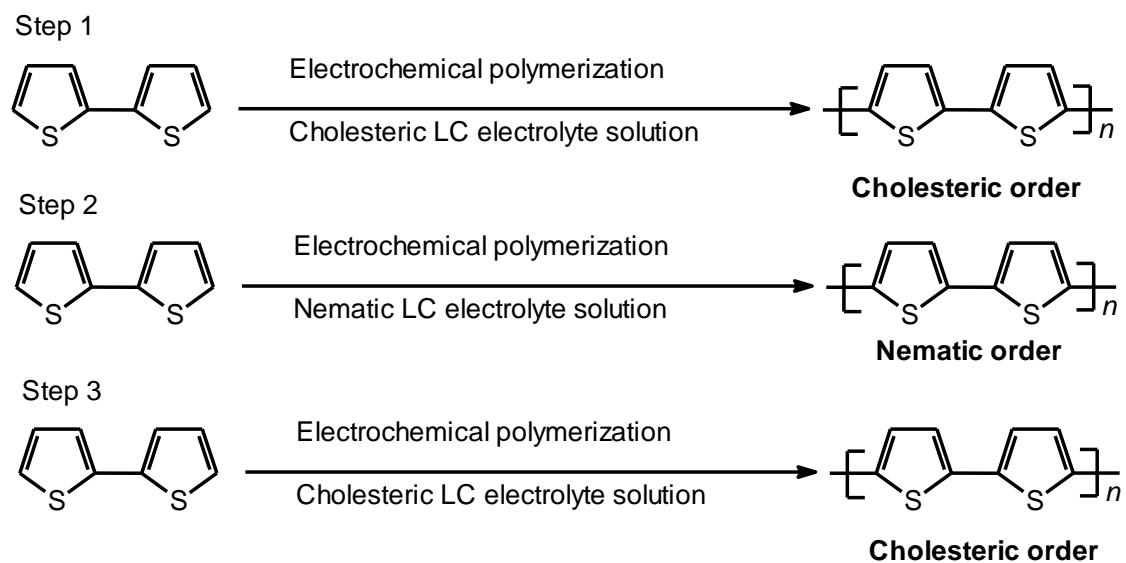
Figure 1. Differential scanning calorimetry (DSC) results for nematic liquid crystal (LC) electrolyte solution (a) and cholesteric LC electrolyte solution. Scan rate = 10 °C/min. These LC electrolyte solutions contain monomer solution (b), supporting electrolyte (salt), chiral inducer (in cases with cholesteric LC). N = nematic, Iso = isotropic, Cr = crystal, Iso* = isotropic (chiral), Ch* = cholesteric, Cr* = crystal (chiral).

Stepwise electrochemical polymerization

A stepwise LC electrochemical polymerization was carried out to obtain a cholesteric-nematic-cholesteric ordered film (Scheme 1). Firstly, polymerization of bithiophene (BT) in cholesteric LC was performed in the sandwich cell. After 30 min, the polymerization cell was disassembled. The film with cholesteric order deposited on the anode side of the ITO was washed with THF and acetone.

After drying the cell, the sandwich cell was re-assembled. Then nematic electrolyte solution containing BT as a monomer was injected into the cell by the capillary method. The polymerization cell was heated to ca. 60 °C and then gradually cooled to 20 °C to obtain the Schlieren texture of the nematic phase. Subsequently, constant voltage (4 V) was applied across the cell. After 30 min, the polymerization cell was disassembled, and the resultant film was washed with THF and acetone and THF.

Next, the sandwich cell was reassembled (the cholesteric-nematic film on the ITO as the anode side). The cell containing the cholesteric LC electrolyte solution with BT was heated and gradually cooled to obtain the fingerprint texture. Then, 4 V was applied across the cell. After 30 min, the cell was disassembled, and the polymer film was washed with THF and acetone to yield a cholesteric-nematic-cholesteric ordered polybithiophene film abbreviated as PBT(Ch*-N-Ch*). Liquid crystallinity of the LC electrolyte solutions after the polymerization was confirmed by visual inspection with polarizing optical microscope (POM). This result indicates that the polymerizations were carried out in the LC. The polymerization progresses with phase separation from the matrix LC during the electrochemical reaction. IR measurements for the polymer thus obtained in the LC indicate no CN and C=O absorption bands, while an absorption band of C=C stretching of the thiophene ring was observed at 1326 cm⁻¹. These results suggest that the polymer contains no 6CB and no chiral inducer except the electrolyte (TBAP, 1033 cm⁻¹) (Fig. 2). The electrolyte has strong interaction with the π -conjugated main chain because of the doping of the polymer (charge transfer-type interaction). Thus, the purification process by washing after polymerization can not remove the TBAP (in the form of ions) from the polymer.



Scheme 1. Stepwise electrochemical polymerization in cholesteric LC, nematic LC, and cholesteric LC to obtain three layers consisting of homo-polymer with different morphology (LC = liquid crystal).

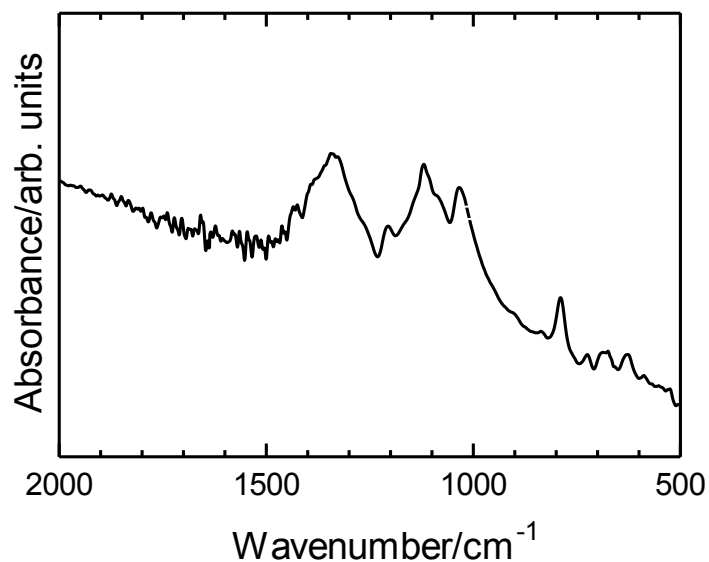


Figure 2. IR absorption spectrum of the triple-layered (Ch*-N*-Ch*) polybithiophene.

Results and discussion

Optical structure

POM images of the top layer (cholesteric order), middle layer (nematic order), and bottom layer are shown in Fig. 3(a). The top layer shows a fingerprint texture consisting of a wire-screen-like structure, as shown in Fig. 3(a, left). The middle layer displays Schlieren texture (Fig. 3(a) middle), and the bottom layer fingerprint texture (Fig. 3(a) left). Fig. 3(b) shows the POM image of the entire region (an edge part of the sample on the ITO) of PBT(Ch*-N-Ch*). This sample was prepared by sliding the Teflon spacer slightly at each step of the polymerization to afford the visible three layers. Fig. 3(c) shows an illustration of the side view of the three-step structure possessing the cholesteric-nematic-cholesteric order. Fig. 4 shows a surface image of the polymer prepared in cholesteric LC electrolyte solution at 30-350 °C. The fingerprint texture of the polymer was not changed due to the heat treatment, but the surface color of the polymer was gradually changed to bright with increase of temperature, confirmed by visual inspection. This result indicates that the polymer shows thermochromism in the film state, and the fingerprint structure is derived from intrinsic surface structure of the polymer, which was transcribed from the cholesteric LC electrolyte solution in the polymerization reaction.

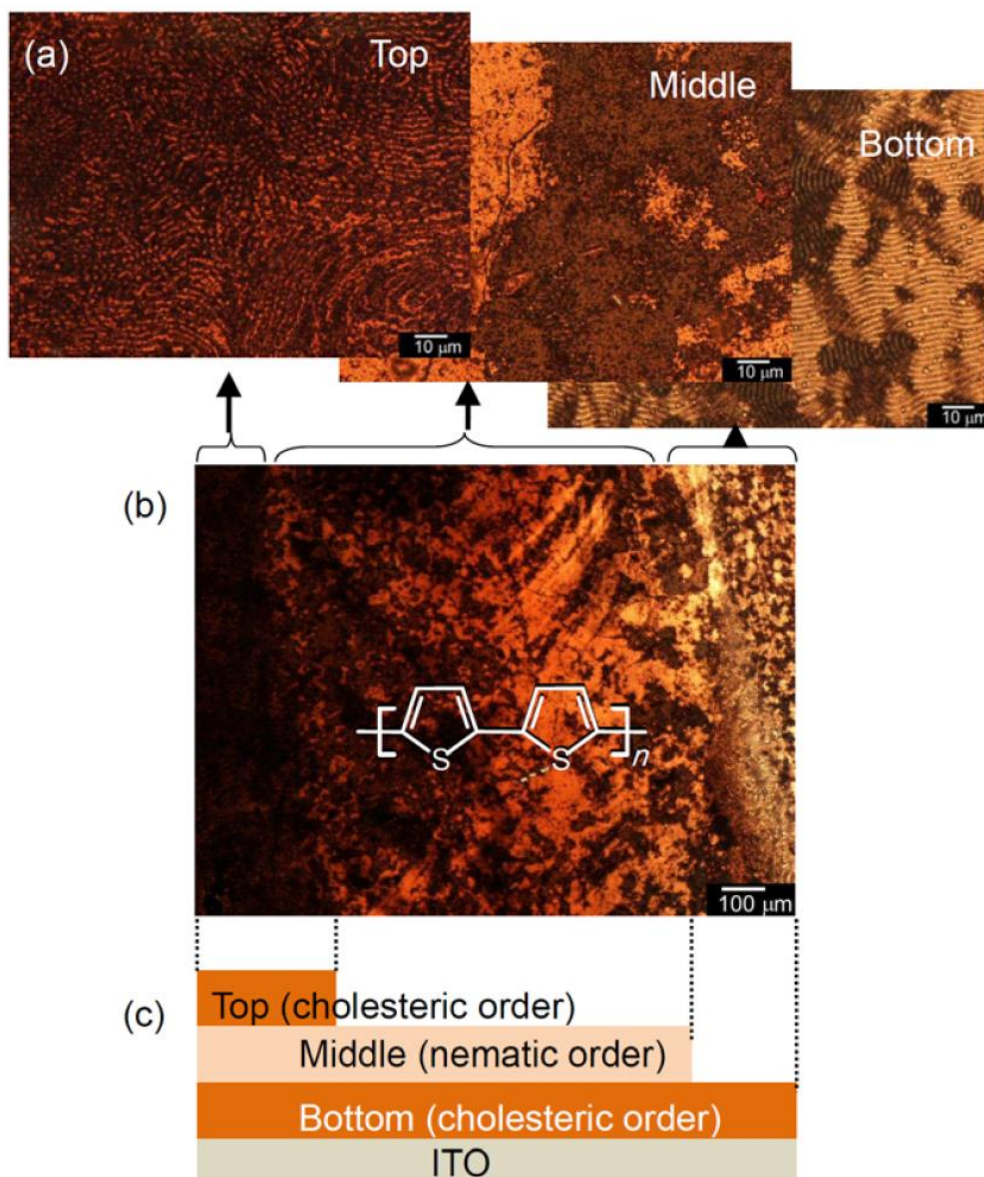


Figure 3. (a) Polarized optical microscopy (POM) image of triple-layer structure of polybithiophene prepared in [cholesteric LC]–[nematic LC]–[cholesteric LC] (PBT(Ch*–N–Ch*)) (reduced state, dedoped). Left (top layer), middle (middle layer), right (bottom layer). (b) POM image of entire region (an edge part of the sample on the ITO) of PBT(Ch*–N–Ch*). (c) Illustration of side view of stacking layers.

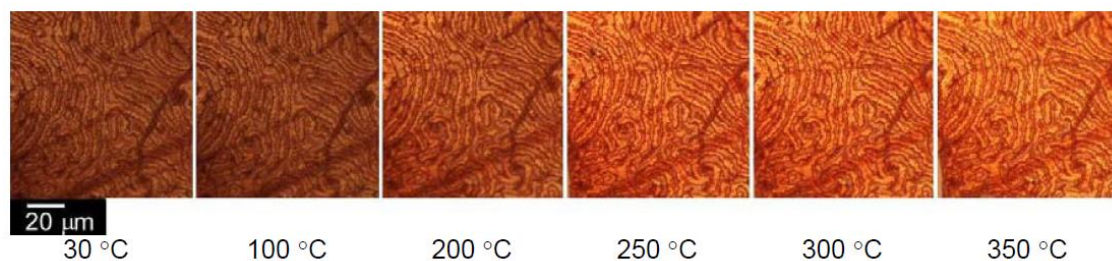


Figure 4. Surface images of polymer prepared in cholesteric liquid crystal electrolyte solution at 30-350 °C.

Electrochemical properties

Cyclic voltammetry measurements of the triple-layer film in the 0.1 M TBAP/acetonitrile solution vs. the Ag/Ag^+ reference electrode shows clear redox behavior at various scan rates (10–50 mV/s), as shown in Fig. 5. The PBT($\text{Ch}^*\text{-N-Ch}^*$) was electroactive and adhered well to the ITO electrode. Fig. 6(a) shows changes in optical absorption at 500 nm (an absorption band of the $\pi\text{-}\pi^*$ transition of the main chain) with applied voltage between 0 – 1 V. The measurement cell included a platinum wire as the counter electrode, an Ag/Ag^+ reference electrode, and the PBT($\text{Ch}^*\text{-N-Ch}^*$) deposited on ITO. The polymer shows optical switching as a function of applied voltage. As seen in Fig. 6(b), the natural color appearance in the International Commission on Illumination (CIE) color space chromaticity diagram, as calculated from the optical absorption spectra of the polymer, indicates that the color of the polymer at each applied voltage shifts toward blue with progressive electrochemical doping.

The change in visible to near-infrared (vis–NIR) optical absorption upon electrochemical reduction (dedoping) at 0 V vs. Ag/Ag^+ reveals a broad absorption maximum at 500 nm corresponding to the $\pi\text{-}\pi^*$ transition of the main chain. The intensity of this peak decreases with increasing voltage, accompanied by the emergence of a new absorption maximum at around 719 nm and an absorption band in the red-to-NIR region at around 1050 nm attributable to the generation of polarons (radical cations) and bipolarons (dications) on the π -conjugated main chains, respectively (Fig. 7(a)).²³ Inset of Fig. 7(a) shows absorption spectra of the polymer at long wavelengths. The chemical structures of polarons and bipolarons are shown in Scheme 2.

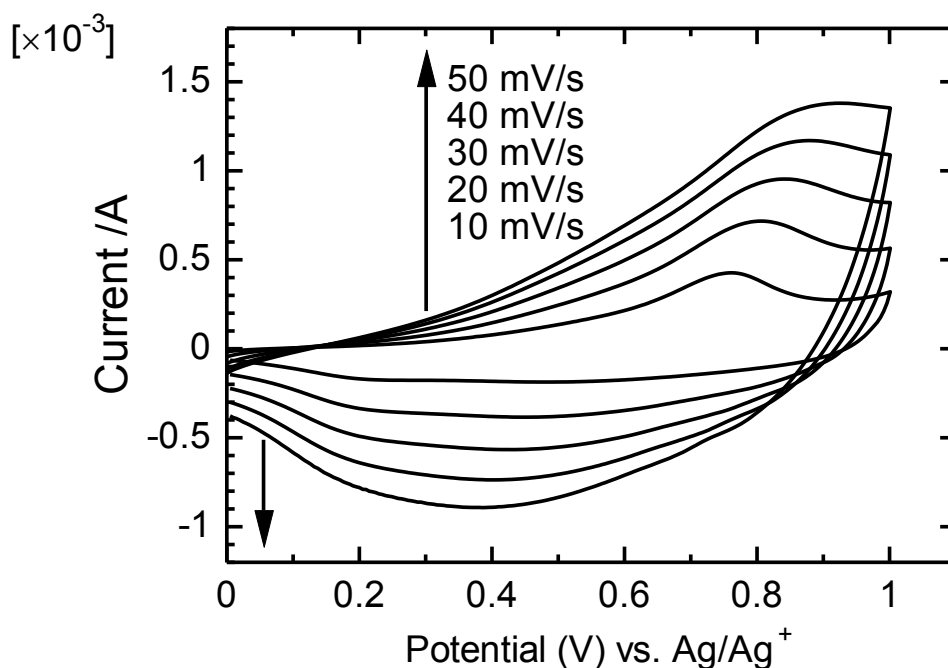


Figure 5. Cyclic voltammogram (CV) of PBT(Ch*-N-Ch*) in a monomer-free 0.1 M TBAP/acetonitrile solution at various scan rates.

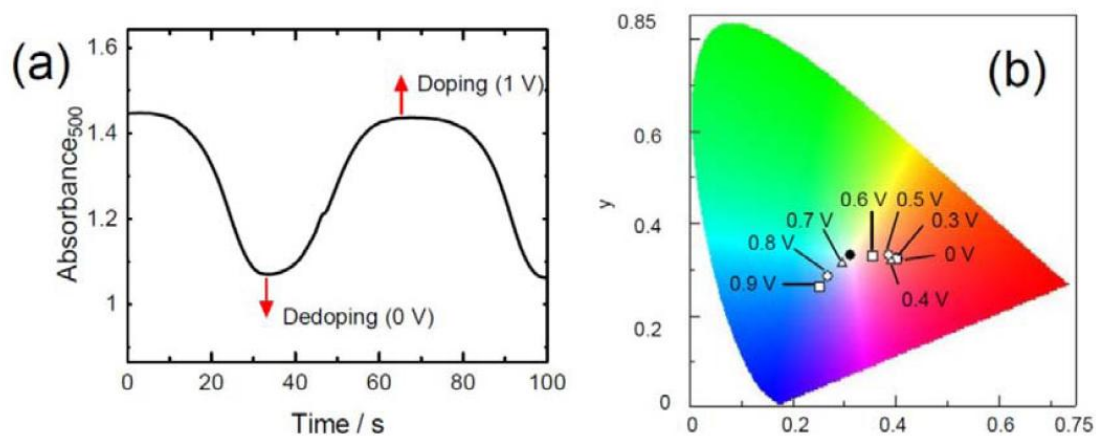


Figure 6. (a) Changes in optical absorption of PBT(Ch*-N-Ch*) film at 500 nm between 0 V and 0.9 V (vs. Ag/Ag⁺ reference electrode) in monomer-free 0.1 M TBAP/acetonitrile solution. (b) CIE color space chromaticity diagram of PBT(Ch*-N-Ch*) film taken as a function of level of electrochemical oxidation (0 V to 0.9 V vs. Ag/Ag⁺).

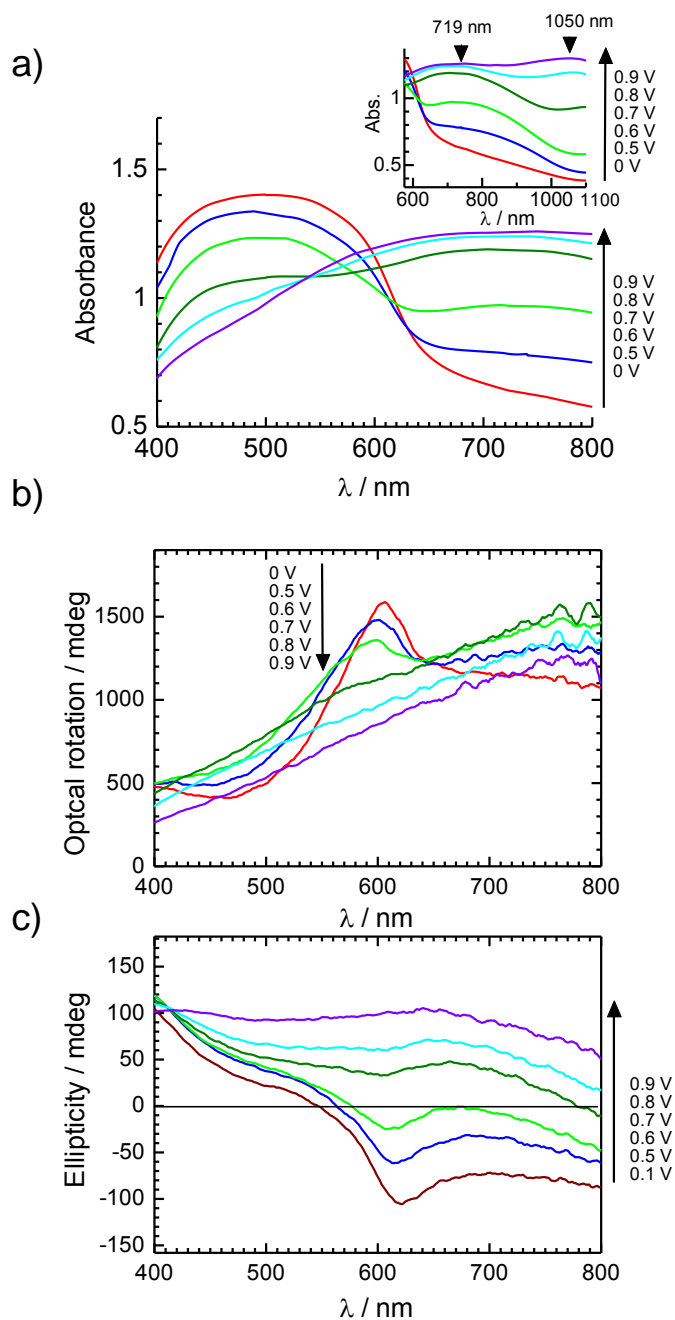
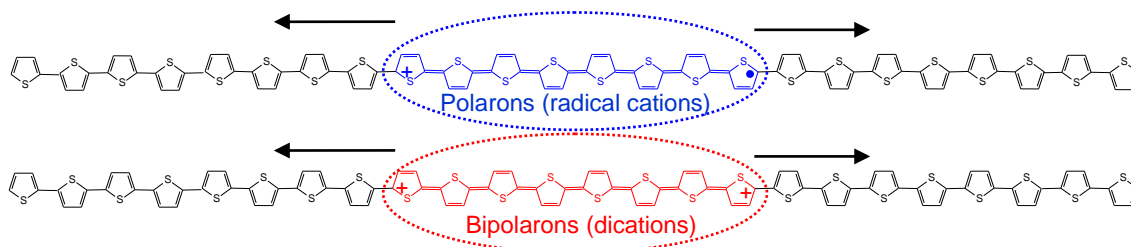


Figure 7. (a) Optical absorption of monomer-free triple-layer PB1(Ch*-N-Ch*) film at various potentials vs. Ag/Ag⁺ reference electrode. Inset shows the absorption spectra (0.9 V) at the long wavelengths. (b) Optical rotatory dispersion (ORD), (c) circular dichroism (CD).



Scheme 2. Chemical structure of polarons and bipolarons for polythiophene.

Redox-driven change in chiroptical activities

Optical rotatory dispersion (ORD) of the polymer as a function of applied voltage vs. an Ag/Ag⁺ reference electrode in 0.1 M TBAP/acetonitrile solution is shown in Fig. 7(b). Upon doping (increase in the applied voltage), the optical rotation at 605 nm decreased. The optical rotation at 480 nm first increased and then decreased with increase of the applied voltage. Absorption at long wavelengths assignable to a polaron band increased with applied voltage. Fig. 8 shows optical rotation at 605 nm and 756 nm vs. applied voltage. This result indicates that the polymer is electro-chiroptically active and that the optical rotation can be tuned via the electrochemical doping process. The optical rotation of the polymer during voltage scanning from 0 V to +0.9 V undergoes repeatable changes at 605 nm. This change in optical rotation demonstrates repeatability of electro-chiroptical chromism.

In situ circular dichroism (CD) spectra of the PBT(Ch*-N-Ch*) films were obtained at 0.1 - 0.9 V. As shown in Fig. 7(c), PBT(Ch*-N-Ch*) exhibits the Cotton effect. In the oxidized state, the CD spectra of the PBT(Ch*-N-Ch*) film display the decrease in intensity of a positive Cotton effect at 377 nm and a negative Cotton effect at 620 nm. The long wavelength signal of PBT(Ch*-N-Ch*) is shifted by ca. 20 nm to long wavelengths as compared with that of a mono-layer film of PBT (Ch*).²⁵ The CD signals cannot be attributed to the chiral inducer employed in the polymerization because the weak Cotton effect of the chiral inducer (Ch*-PEL) is only observed at short wavelengths (240–340 nm). This result indicates that the circular dichroism of PBT(Ch*-N-Ch*) can be changed by adjusting the conditions of the electrochemical redox process. The CD spectra show positive signal at high voltage. The dopant ion (ClO₄⁻) intrudes between the main chains and releases inter-main chain helical

aggregation to decrease the helicity in the doped state. Furthermore, generation of polarons and bipolarons by doping through application of voltage forms relatively planar structures in the main chains, which depresses formation of intra-main chain helical structure.

Exoskeleton of beetles with cholesteric-nematic-cholesteric order reflects circular polarized light by using multilayer structure. As for the multilayer polymer film thus prepared in this study is comparable to reflection functionality of the photonic insects. If the multilayer film light reflection function in the manner of natural photonic insects having multilayered LC order, the top layer of the film with cholesteric order reflects right-handed circular polarized light (R-CPL), and left-handed circular polarized light (L-CPL) passes through the top layer upon incidence of light (R-CPL + L-CPL). Subsequently, the middle layer with nematic order converts L-CPL into R-CPL. Finally, bottom cholesteric ordered layer reflects R-CPL at visible range. Therefore, the CD shows negative signals (right-handed polarized direction), as a result of gain loss due to reflection of R-CPL light at visible range at low voltage (dedoped state). The gain loss due to reflection and absorption appears to be the CD signals. In the doped state, helicity of the cholesteric ordered layer is changed, and R-CPL was reflected from the polymer. This may not be perfect for the PBT(Ch*-N-Ch*) with fingerprint pattern (homogeneous structure, helical axis is parallel to the layer) because this process is effective for Grandjean cholesteric LC order (planar structure, helical axis is perpendicular direction to the layer). The triple-layer polymer thus prepared in this study can reflect R-CPL, and L-CPL passes through the film. Simultaneously, optical absorption occurs. Optical rotation of the triple-layer polymer occurs only left direction (positive values in the ORD), as shown in Figure 7(c). The reflections of R-CPL at low voltage and L-CPL at high voltage are based on Ch*-N-Ch* order, which can be dominant factor for the CD and the ORD. However, the incompleteness of the light reflection functionality of the triple layer polymer may pass L-CPL as an output. The trough of the CD corresponds to peak top of the ORD signal, although a maximum in the ORD corresponds to inflection point in the CD in general. The CD and ORD signals do not always correspond to the optical absorption in the triple-layer polymer in the present case. Optical absorption of the polymer removes a certain wavelength range of reflection light.

The functional reflection derives from the layered structure containing helical structure of the polymer and optical absorption of the π -conjugated main chain. In addition, the polymer has no chiral center. The chiroptical activity comes from one-handed helical structure of main chain and helical π -stacking aggregation structure

between the main chains.

Refractive index (n) of the triple-layer polymer (as prepared form) shows a maximum at 537 nm. This wavelength corresponds to inflection points of the CD and the ORD of the polymer.

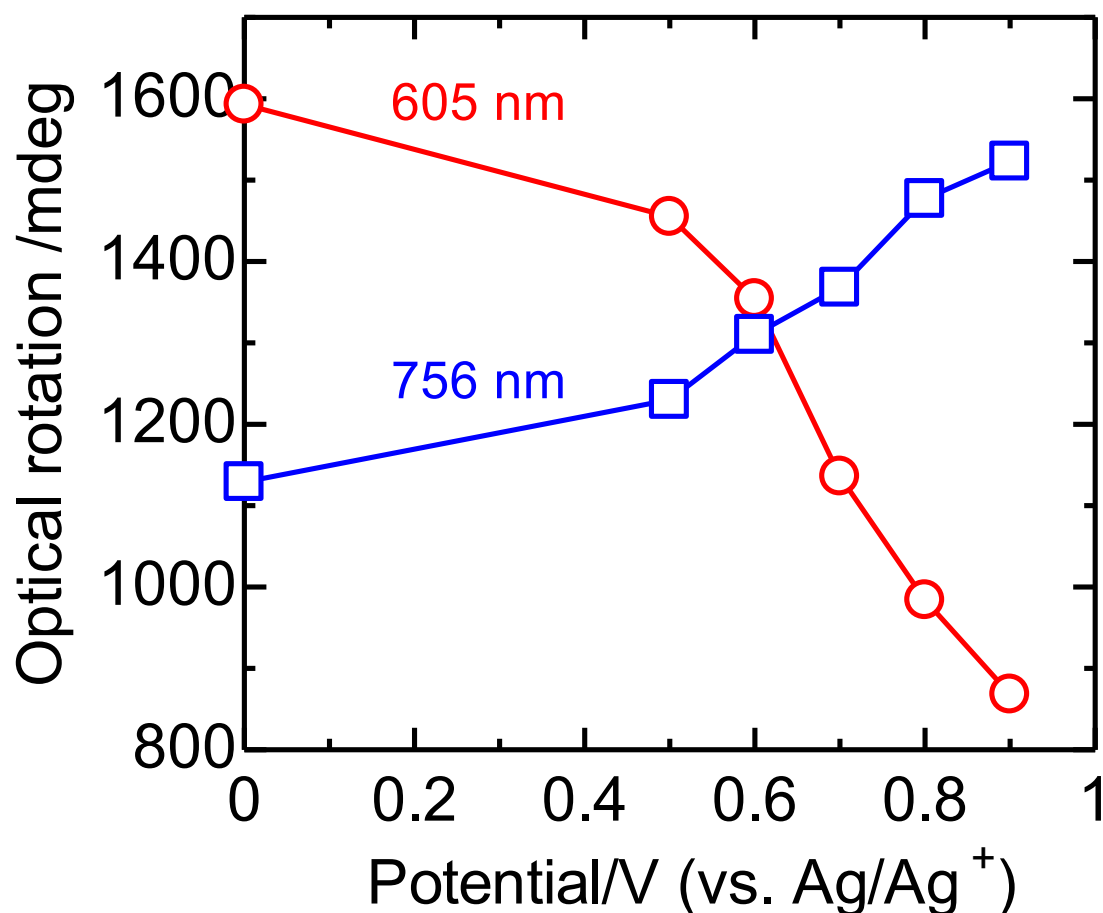


Figure 8. Optical rotation of triple-layer PBT(Ch*-N-Ch*) film at 605 nm and 765 nm as a function of application potentials vs. Ag/Ag⁺ reference electrode.

Structural color

The multi-layer structure of a polymer can produce selective reflection of light. The multi-layer polymer in this study has such an alternation order. However, thin layers are required for transparency in the multi-layer polymer for obtaining clear selective light reflection. Thickness of the polymer film obtained in cholesteric liquid crystal electrolyte solution (polymerization time = 30 min) is 100–300 nm. Therefore, the

stepwise electrochemical polymerization of the monomer in LCs was carried out over short times to yield thin layers with LC order. The bottom layer (polymerized in cholesteric LC) and middle layer (polymerized in nematic LC) were prepared by electrochemical polymerization for 2 min with 4 V, and the top layer (polymerized in nematic LC) was synthesized for 3 min with 4 V. This procedure produced a polybithiophene thin film with [cholesteric]-[nematic]-[cholesteric] orders.

The surface profile of the triple-layer system was confirmed with a non-contact scanning white-light interferometer, indicating that the film consists of three layers (each layer thickness ~10 nm). Fig. 9(a) shows the structural color of this polymer (reduced state) under obliquely incident white light. The film shows turquoise blue reflection color due to selective reflection of light. On the other hand, the natural appearance and transmission color (shadow, Fig. 9(a)) is red. This character is comparable to that of Morpho butterflies, which show blue structural color and brown transmission color.

The change in surface structural color of the present polymer during redox cycling is displayed in Fig. 9(b–g). The natural color of the polymer changes from red to blue (Fig. 9(b–d)) with the oxidation process, while the structural color changes from turquoise-blue to ocher under oblique white light (Fig. 9(e–g)). In this case, the white light irradiates the top region of the sample. Therefore, the lower region of the sample in Fig. 9(e) shows natural appearance (red). This result suggests that the structural color derived from multi-layer interference can be tuned by the redox process based on an electrochemical doping-dedoping mechanism. Refraction and reflection indices can be changed by the redox process accompanied by change in the electronic structure of the polymer with the electrochemical redox cycle. These changes in physical properties produce change in total interference reflection color for the multi-layer polymer. This result implies that the present study presents an approach for production of tunable artificial color similar to Morpho butterflies based on a multi-layer system of organic semiconductor with liquid crystal order.

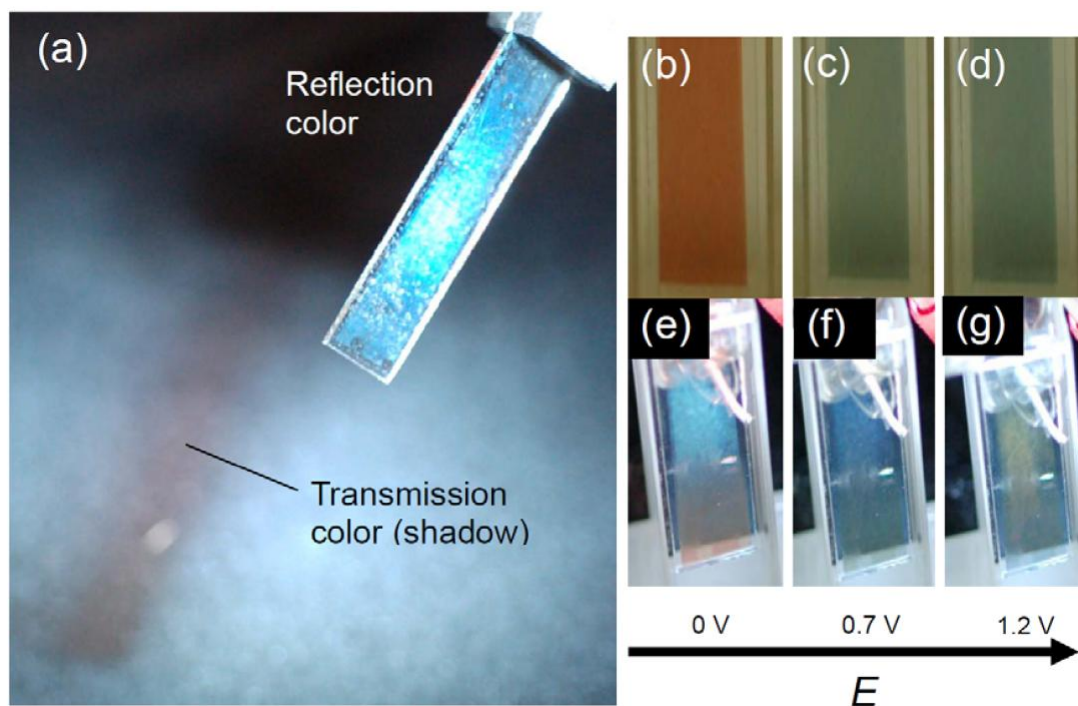


Figure 9. (a) The multi-layer polymer film on ITO under white-light oblique incidence. Natural appearance electrochromism (b-d) and reflection electrochromism under white-light oblique incidence (the light was incident on the top part of the sample) (e-g) of the polymer in 0.1 M TBAP/acetonitrile solution at 0 V, 0.7 V, and 1.2 V vs. Ag/Ag^+ reference electrode.

Surface structure of the Morpho butterfly and multi-layer polymer film with LC order

Scales of Morpho butterflies have characteristic micro-structure, as shown in Fig. 10(a). The scales have many vertical vanes (ridges) with lamellar structure.²⁴ The substrate (bottom cuticle) contains pigment for enhancement of blue color. The scales reflect light with diffraction by their grooved structure. Interference of light occurs due to the multi-layer interference system with a lamellar structure in the horizontal direction.^{16(c)} The combination of diffraction, interference, and pigment color beneath the iridescent scales allows beautiful blue-colored reflection. The polymer with multi-layered structure possesses some analogous points of the scale of the Morpho butterfly. Firstly, the multi-layer structure consisting of cholesteric-ordered layer and nematic-ordered layer can show interference of light. In this case, oblique incidence is required because of small the layer thicknesses. Next, the sequential dielectric structure with periodicity of the surface of the polymer, produced by transcription from

cholesteric LC, can function as a diffraction grating. Although the individual polymer molecules have no directors, cholesteric LC-like periodic structure is produced by the polymerization in cholesteric LC and nematic LC. The helical half-pitch of cholesteric LC corresponds to the helical half-pitch of the resultant polymer prepared in cholesteric LC. Orientation direction of the individual main chain (polymer) is described with bi-directional arrow in Fig. 10(b). The periodicity functions as a diffraction grating. The two functions (interference, diffraction) display turquoise-blue reflection. Furthermore, the controllable color of the polymer based on redox cycling allows tunability of the reflection color. The inherent color of the polymer is comparable to the pigment in the scales of the butterflies.

Note that single conjugated polymer films with LC orders shows diffraction and rainbow colors (seven colors) upon irradiation of oblique incident of light.²⁵ A conjugated polymer having smectic A like layer structure shows blue color.²⁶ Multilayer textiles showing rainbow color has been developed.²⁷

Advantage of the multi-layer film compared to single conjugated polymer films with LC orders in this study is exhibition of mono-color via combination of multi-layer interference and diffraction. Stepwise sandwich cell electrochemical polymerization allows preparation of the multi-layer film with LC order showing so-called "Morpho color".

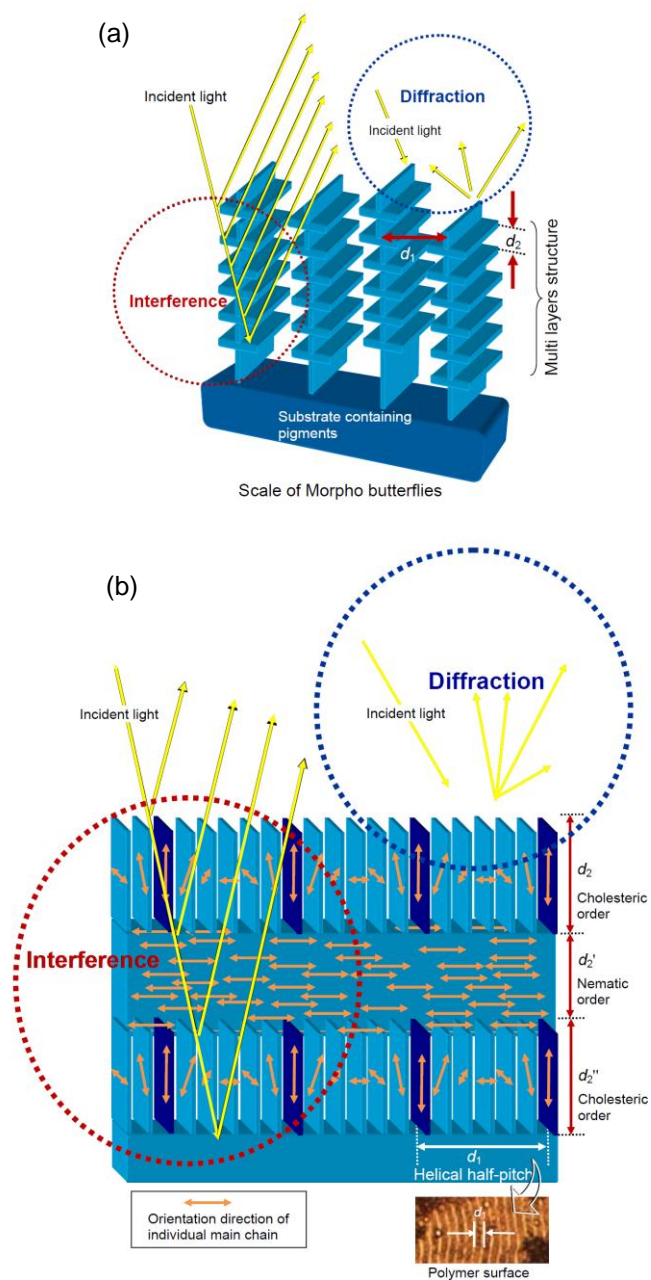


Figure 10. (a) Diffraction and interference behavior of structural color of the scales of the Morpho butterfly. d_1 is inter-layer distance in the horizontal direction, d_2 is the intra-layer distance between lamellae in the perpendicular direction. $d_1 = 80\text{--}140$ nm, $d_2 = 50$ nm. (b) Proposed multi-layer structure of the polymer produced in cholesteric liquid crystals and nematic liquid crystals, and light diffraction and interference behavior. d_1 is the helical pitch of the polymer prepared in cholesteric liquid crystal. d_2 , d_2' , and d_2'' are layer thickness of the polymer. Bi-directional arrows indicate orientation direction of polymer molecules. ITO = indium-tin-oxide.

Conclusions

The liquid crystal sandwich-cell polymerization method allows preparation of optically active films with LC order. The method can be further applied for preparation of optically active conjugated polymer laminate films. The stepwise polymerization produces triple-layer films consisting of [cholesteric LC order]-[nematic LC order]-[cholesteric LC order]. This method realized preparation of a multi-layer structure from one kind polymer with differing molecular orientations in each layer.

The multi-layer polymer shows turquoise-blue structural color via interference and selective reflection of light in obliquely incident white light. The artificial laminated π -conjugated polymer film with LC order thus synthesized further shows redox-driven change in chiroptical activities and tunable structural color. This method may be referred to as structure organizing polymerization.

Acknowledgments

The author is grateful to the Engineering Workshop of the University of Tsukuba for glasswork. This research was supported by the Japan Society for the Promotion of Science (JSPS), Grant-in-Aid for Scientific Research, 22550161.

Techniques

All monomer syntheses were performed under argon atmosphere using Schlenk/vacuum line techniques. Optical absorption spectra were obtained using a UV-Vis spectrophotometer (Hitachi U-2000 and Jasco V-600). Circular dichroism (CD) and optical rotation dispersion (ORD) measurements were performed using a Jasco J-720 spectrometer with an ORDE-307W ORD unit. Electrochemical measurements of polymers were conducted using an electrochemical analyzer (μ Autolab III, Autolab, the Netherlands), and optical textures were observed using a high-resolution polarized microscope (Nikon ECLIPS LV 100) with a Nikon LU Plan Fluor and Nikon CFIUW lenses without oil immersion. Film thickness of the samples was measured with non-contact scanning white-light interferometer, ZYGO New View 5032. Reflective index of the polymer was obtained with a Jasco ARAM-735 system.

Matrix-assisted laser desorption ionization, time-of-flight mass spectroscopy (MALDI-TOFF-MS) measurements were carried out with AB SCIEX TOF/TOF5800 system.

Polymerization condition for thin multi-layer laminate film showing turquoise-blue structural color

Constitution of cholesteric liquid crystal electrolyte solution containing monomer: *n*-Hexyl-cyanobiphenyl (6CB) 0.5 g, tetra-*n*-butyl ammonium perchlorate (TBAP) 2 mg, cholesteryl pelargonate (Ch*-PEL) 100 mg, bithiophene (BT) 40 mg. Helical pitch of the cholesteric LC-containing monomer is 4.9 μm , confirmed by the Cano-wedge method.²⁸ Here, the formula $P = 2a \cdot \tan \theta$ is employed for obtaining the helical pitch (P). The parameters a , and θ are length of Cano-line in the cell, degree of the Cano-wedge, respectively.²⁹

Constitution of nematic liquid crystal electrolyte solution containing monomer: 6CB 0.5 g, TBAP 2 mg, BT 20 mg.

Polymerization

Bottom layer (cholesteric order), 4 V, 2 min at 18 °C. Middle layer (nematic order), 4 V, 2 min. Top layer (cholesteric order), 4 V, 3 min at 16 °C for obtaining the thin film. MALDI TOFF-MS measurement of the polymer indicates that the m/z signals increase with molecular repeat units of bithiophene (= 164.25 g/mol).

References

1. J. Zhang, L.-B. Kong, B. Wang, Y.-C. Luo, L. Kang, *Synth. Met.*, 2009, **159**, 260–266.
2. R. Pokropa, I. Kulszewicz-Bajer, I. Wielgus, M. Zagorska, D. Albertini, S. Lefrant, G. Louarn, Pron A. *Synth. Met.*, 2009, **159**, 919–924.
3. E. Kozma, D. Kotowski, F. Bertini, S. Luzzati, M. Catellani, *Polymer*, 2010, **51**, 2264–2270.
4. W. van Zoelen, S. Bondzic, T. F. Landaluce, J. Brondijk, K. Loos, A.-J. Schouten, P. Rudolf, G. ten Brinke, *Polymer*, 2009, **50**, 3617–3625.
5. M. I. Redondo, M.V. García, E. S. de la Blanca, M. Pablos, I. Carrillo, M. J. González-Tejera, E. Enciso, *Polymer*, 2010, **51**, 1728–1736.
6. Q. Qin, J. Tao; Y. Yang, *Synth. Met.*, 2010, **160**, 1167–1172.
7. K. Ikushima, S. John, K. Yokoyama, S. Nagamitsu, *Smart. Mater. Struct.* 2009, **18**, 095022.
8. A. L. Briseno, S. Han, I. E. Rauda, F. Zhou, C.-S. Toh, E. J. Nemanick, N. S. Lewis, *Langmuir*, 2004, **20**, 219–226.
9. C. Kvarnstrom, R.-M. Latonen, A. Ivaska, *Mat. Res. Soc. Symp. Proc.*, 1997, 451,

- 425.
10. J. L. Boehme, D. S. K. Mudigonda, J. P. Ferraris, *Chem. Mater.*, 2001, **13**, 4469–4472.
 11. D. Aradilla, F. Estrany, E. Armelin, C. Alemán, *Thin Solid Films*, 2010, **518**, 4203–4210.
 12. C. Gu, T. Fei, L. Yao; Y. Lv, D. Lu, Y. Ma, *Adv. Mater.*, 2011, **23**, 527–530.
 13. M. Grzeszczuk, J. Kalenik, A. Kępas-Suwara, *J. Electro. Chem. Soc.*, 2009, **626**, 47–58.
 14. R. A. Potyrailo, H. Ghiradella, A. A. Vertiatchikh, K. Dovidenko, J. Cournoyer, E. Olson, *Nat. Photon.*, 2007, **1**, 123–128.
 15. N. Tamaoki, *Adv. Mater.* 2001, **13**, 1135–1147.
 16. (a) A. E. Seago, P. Brady, J.-P. Vigneron, T. D. Schultz, *J. R. Soc. Interface*, 2009, **6**, S165–S184; (b) J.-P. Vigneron, M. Rassart, C. Vandembem, V. Lousse, O. Deparis, L. P. Biró, D. Dedouaire, A. Cornet, P. Defrancel, *Phys. Rev.*, 2006, **E 73**, 041905.; (c) S. Kinoshita, S. Yoshioka, in: *Structural Colors in Biological Systems – Principles and Applications*; S. Kinoshita, S. Yoshioka Eds.; Osaka University Press: Osaka, Japan, 2005, p. 113-139.
 17. Y. Bouligand, *Tissue Cell*, 1972, **4**, 189–190, 192–217.
 18. (a) H. Goto, *Phys. Rev. Lett.*, 2007, **98**, 253901. (b) H. Yoneyama, K. Kawabata, A. Tsujimoto, H. Goto, *Electrochem. Commun.*, 2008, **10**, 965–969.
 19. (a) P. M. Beaujuge, S. Ellinger, J. R. Reynolds, *Nat. Mater.*, 2008, **7**, 795–799; (b) L. Groenendaal, G. Zotti, P.-H. Aubert, S. M. Waybright, J. R. Reynolds, *Adv. Mater.*, 2003, **15**, 855–879.
 20. G. Sonmez, C. K. F. Shen, Y. Rubin, F. Wudl, *Angew. Chem. Int. Ed.*, **2004**, **43**, 1498–1502.
 21. C.-G. Granqvist, *Nat. Mater.*, 2006, **5**, 89–90.
 22. H. Goto, *J. Mater. Chem.*, 2009, **19**, 4914–4921.
 23. H. Goto, *Mater. Chem. Phys.*, 2010, **122**, 69–72.
 24. S. Kinoshita, S. Yoshioka, Y. Fujii, N. Okamoto, 2002, *Forma*, **17**, 103–121.
 25. (a) H. Goto, *Adv. Func. Mater.*, 2009, **19**, 1335–1342. (b) H. Goto, *J. Electrochem. Soc.*, 2007, **154**, E63–E67.
 26. H. Goto, S. Nimori, *J. Mater. Chem.*, 2010, **20**, 1891–1898.
 27. Caveney, S, *Proc. R. Soc. London*, 1971, **B178**, 205–225.
 28. Yoshimura, M. Iohara, K., Shimizu, S. Tabata, H. 2000, *J. Soc. Fiber Sci. Tech, Jpn.*, **56**, 348–351 (in Japanese).
 29. R. Cano, *Bull. Soc. Fr. Mineral. Cristallogr.*, 1968, **91**, 20–27.

Supplementary information for:

Liquid Crystal Stepwise Electropolymerization – An
Approach for Production of Insects' Photonic Structure

Hiromasa Goto

Division of Materials Science, Faculty of Pure and Applied Sciences,
University of Tsukuba, Tsukuba, Ibaraki 305-8573, Japan

Correspondence to H. Goto, Tel: +81-298-53-5128, fax: +81-298-53-4490
Email: gotoh@ims.tsukuba.ac.jp



Figure S1. Appearance of a blue mountain butterfly (*Papilio Ulysses*).

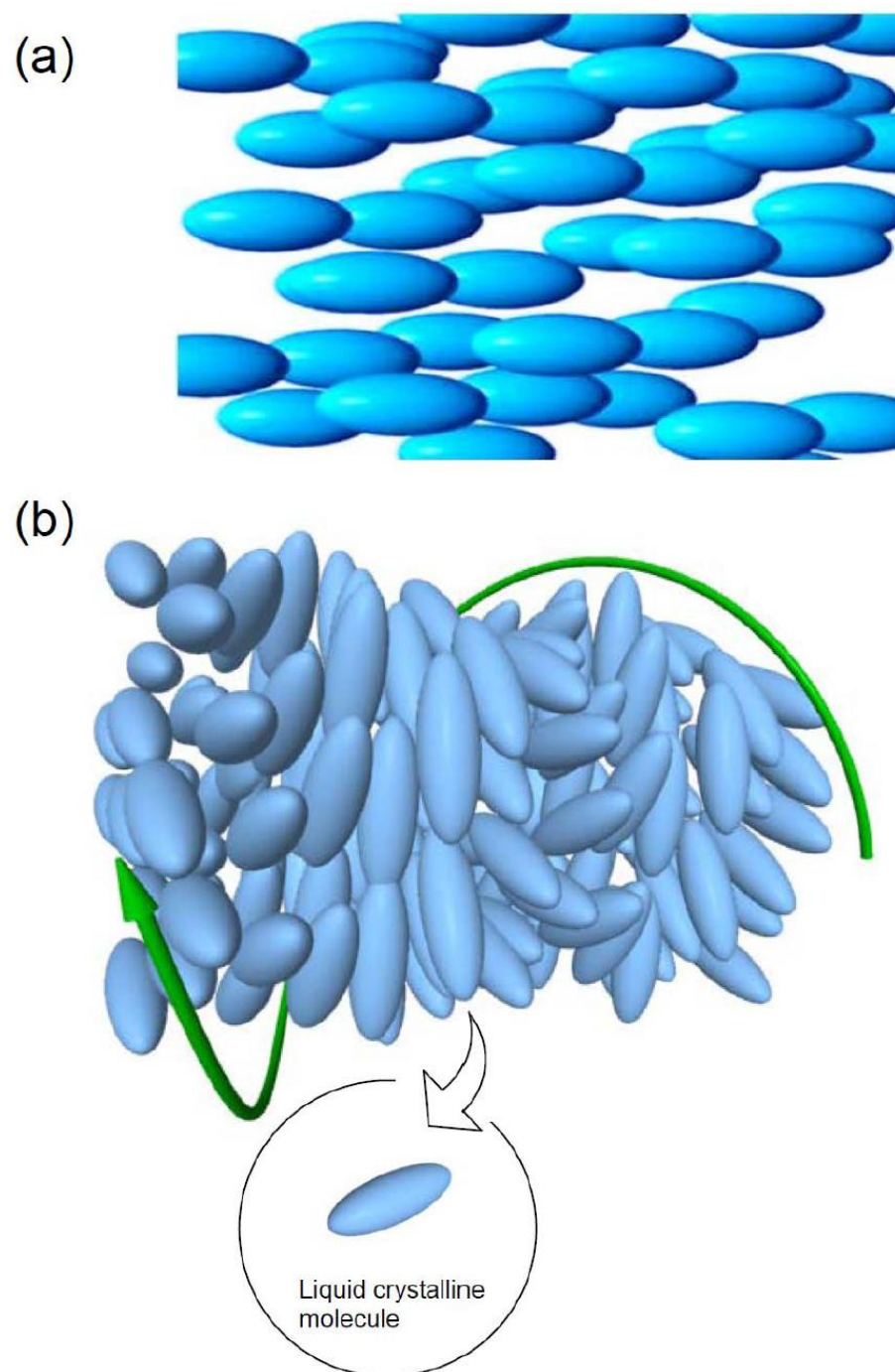


Figure S2. (a) Molecular aggregation structure of nematic phase, and (b) cholesteric phase.

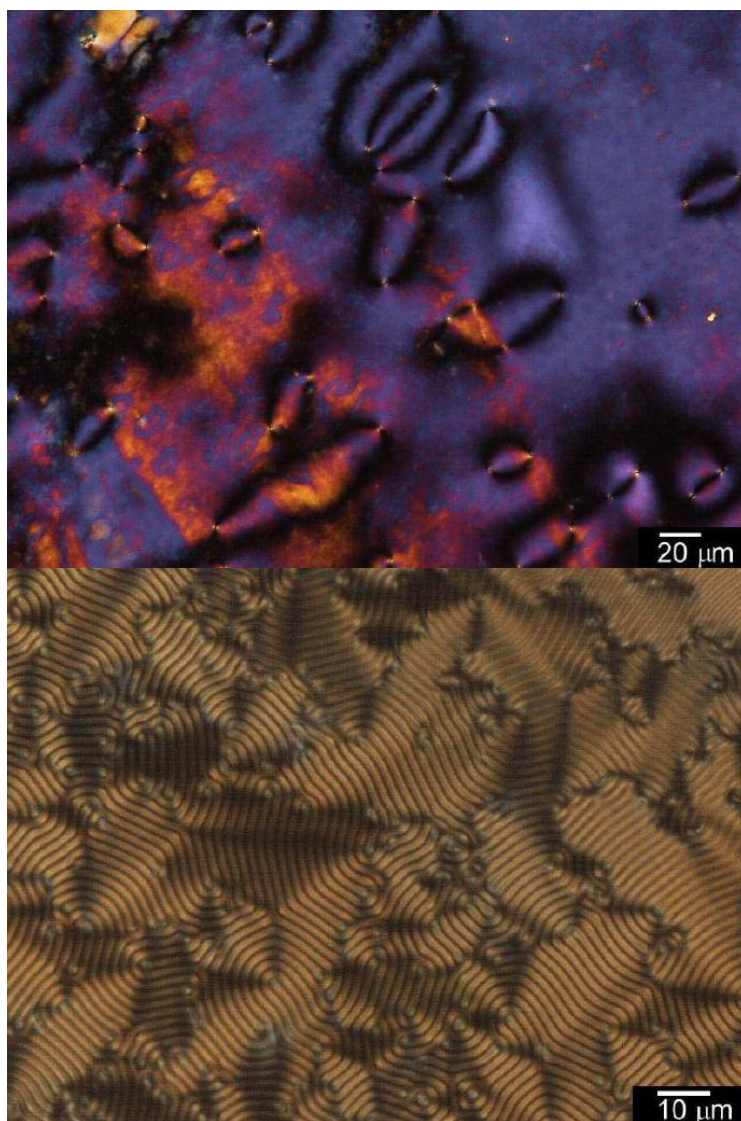


Figure S3. Photographs are polarized optical microscopy images of LC electrolyte solutions. (a) Nematic liquid crystal electrolyte solution, (b) cholesteric liquid crystal electrolyte solution.

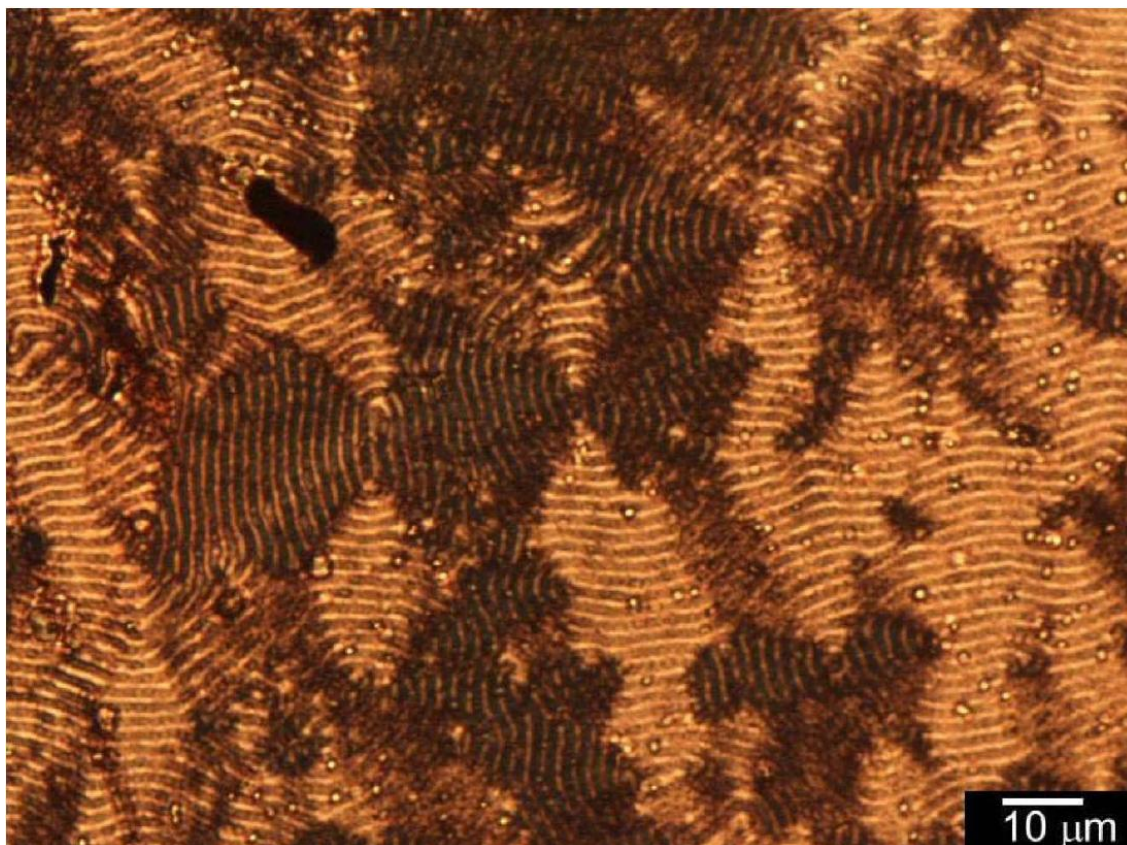


Figure S4. POM image of bottom layer of PBT(Ch*-N-Ch*) in reduced (de-doped) state. 500x.

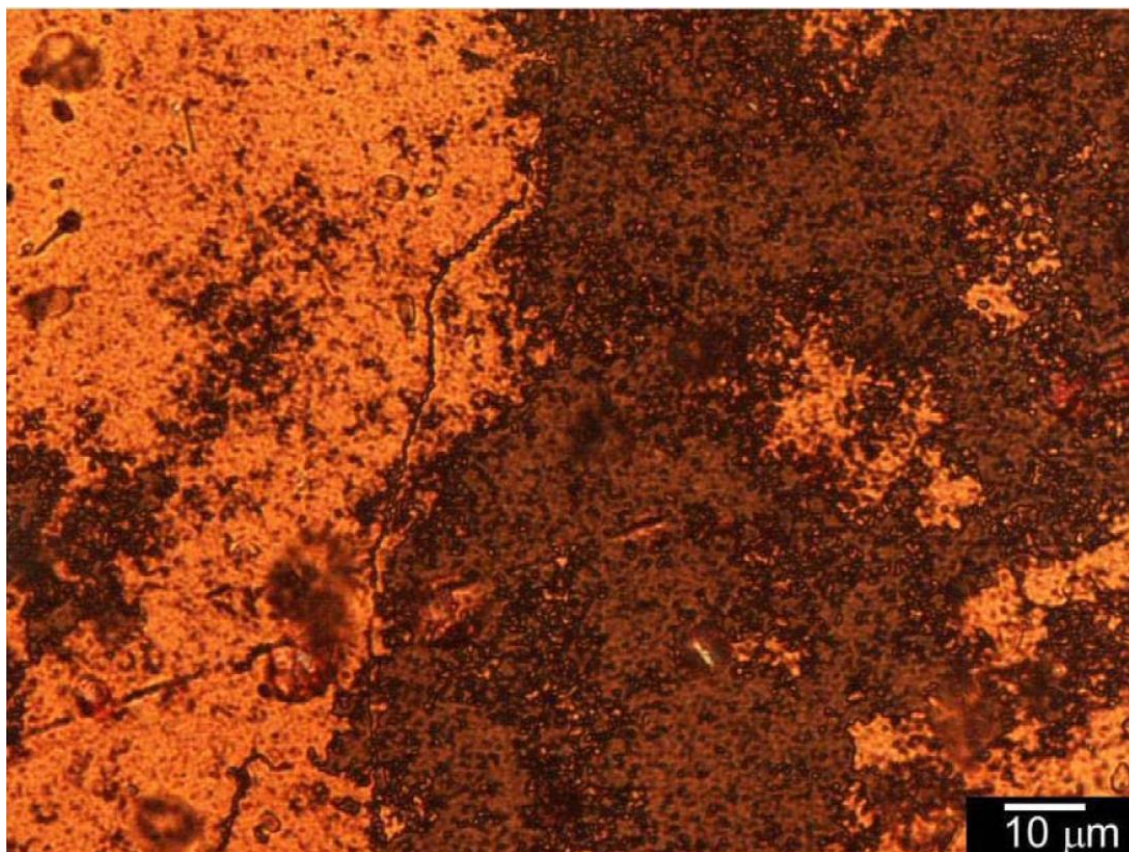


Figure S5. POM image of the middle layer of PBT(Ch*-N-Ch*) in reduced (de-doped) state showing threaded like texture. 500x.

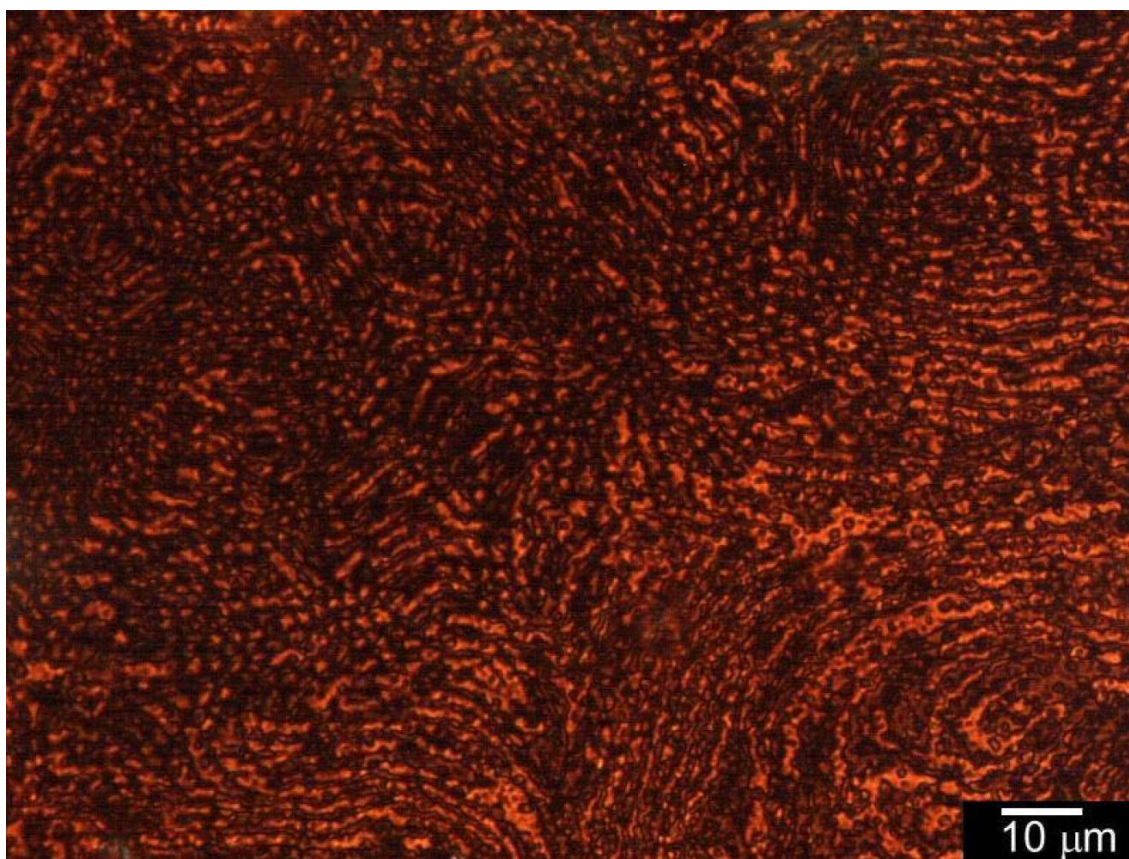


Figure S6. POM image of the top layer of PBT(Ch*-N-Ch*) in reduced (dedoping) state. 500x.

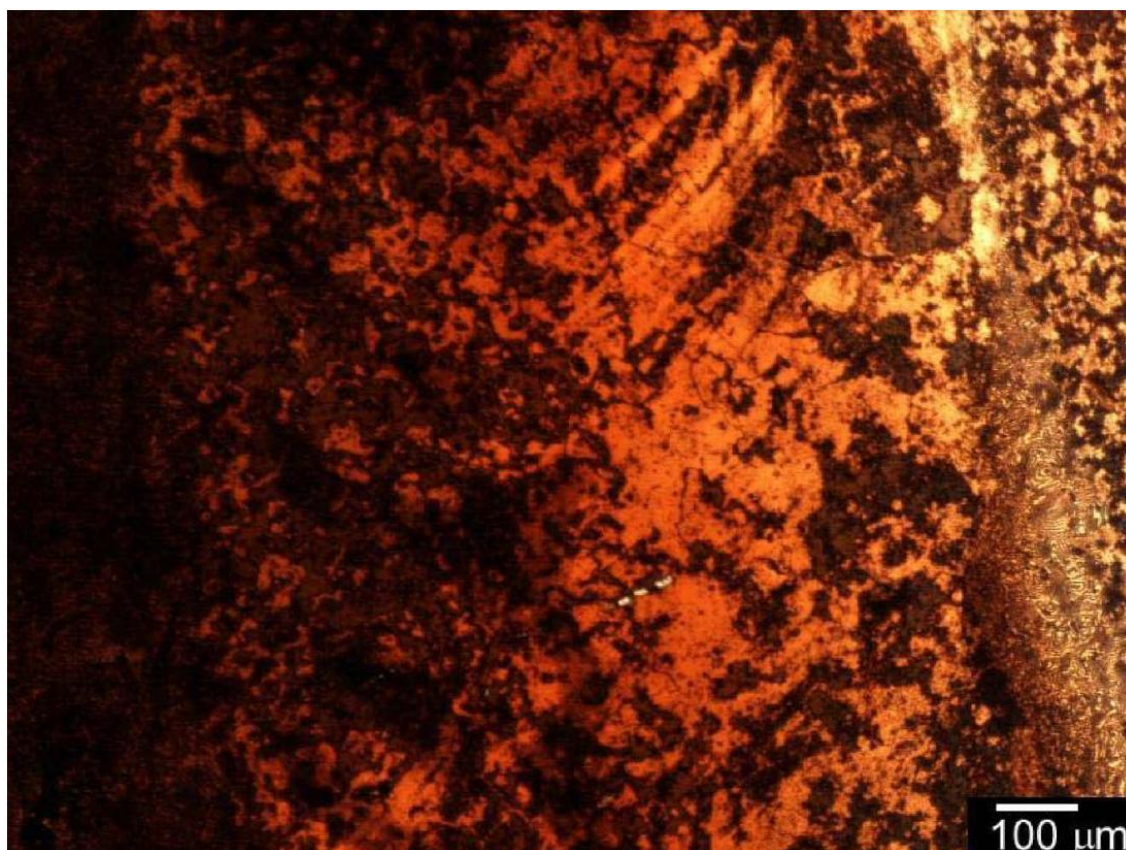


Figure S7. POM image of the entire area (an edge part of the sample on the ITO) of PBT(Ch*-N-Ch*) in reduced (de-doped) state. 500 x.

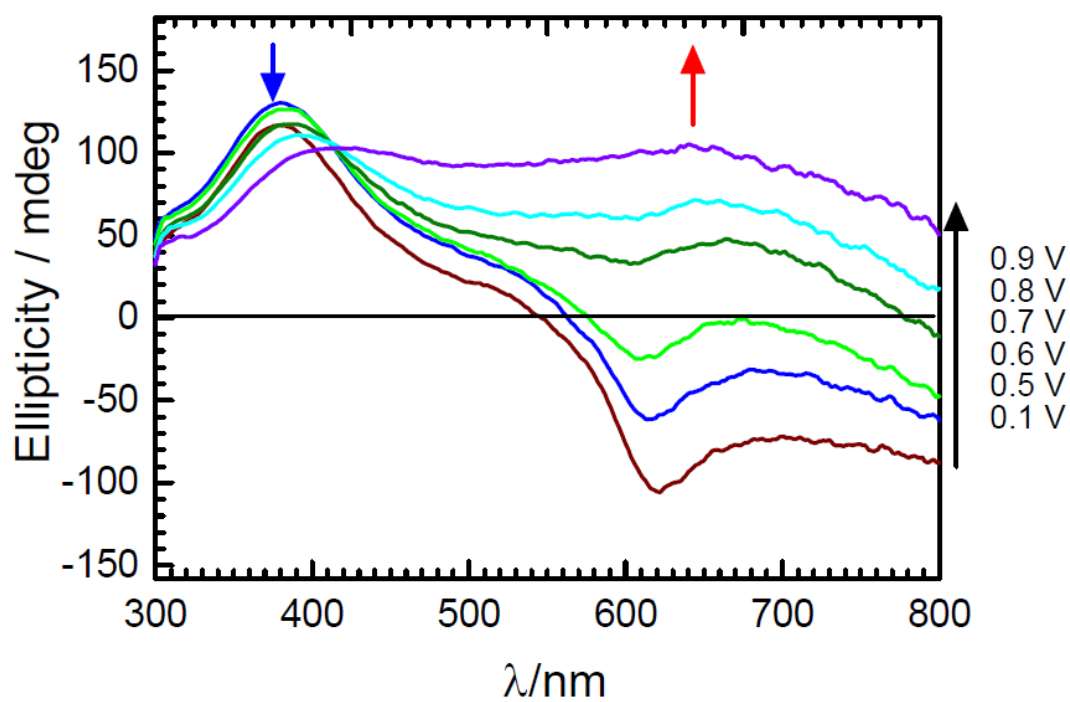


Figure S8. CD spectra of monomer-free triple-layer PBT(Ch*-N-Ch*) film at various potentials vs. Ag/Ag⁺ reference electrode from 300 -800 nm.

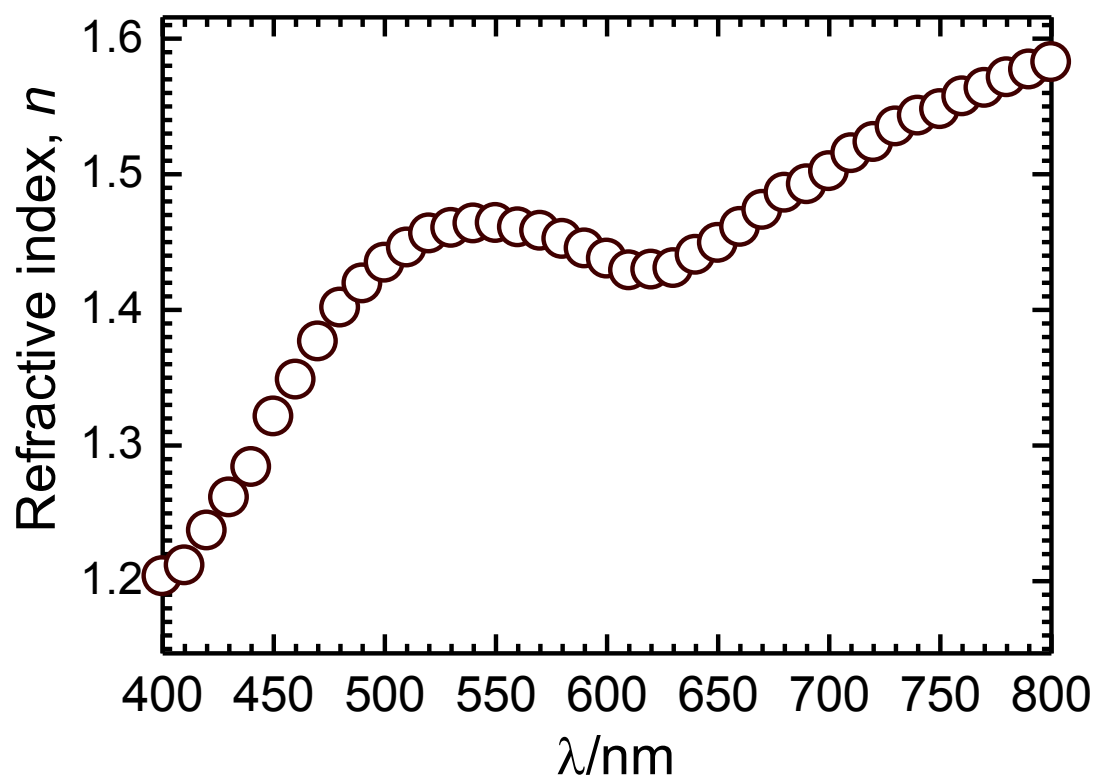


Figure S9. Refractive index (n) vs. wavelength as prepared PBT(Ch*-N-Ch*).

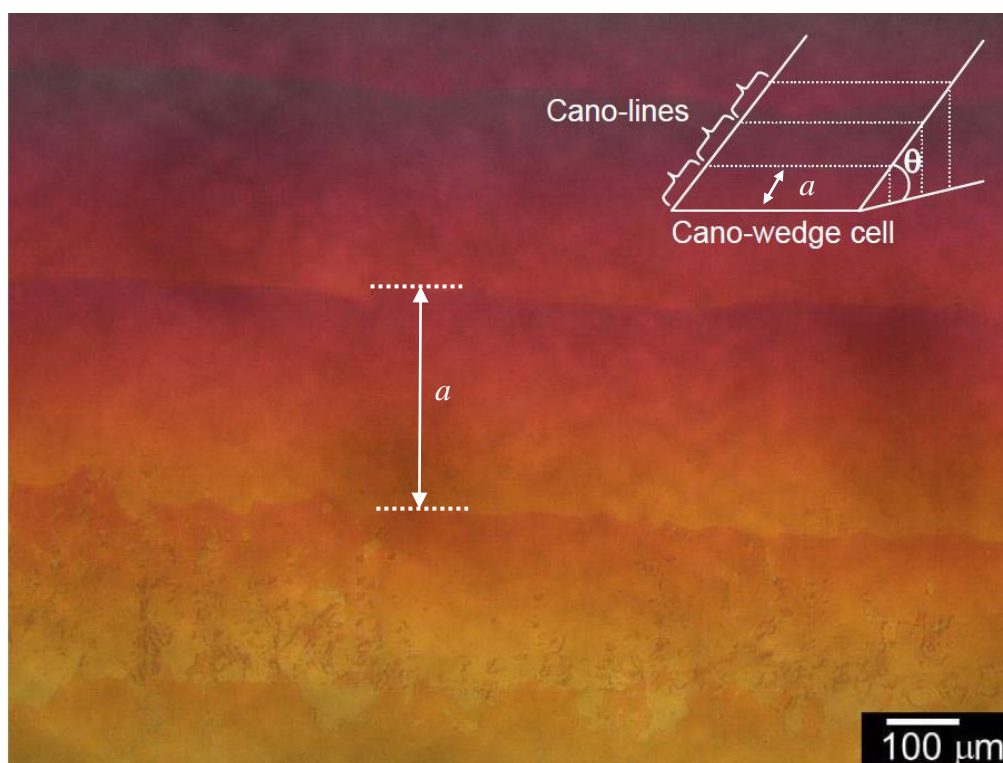


Figure S10. Cano-lines of cholesteric electrolyte solution containing monomer, electrolyte, and the chiral inducer in Cano wedge cell. $a = 294 \mu\text{m}$.

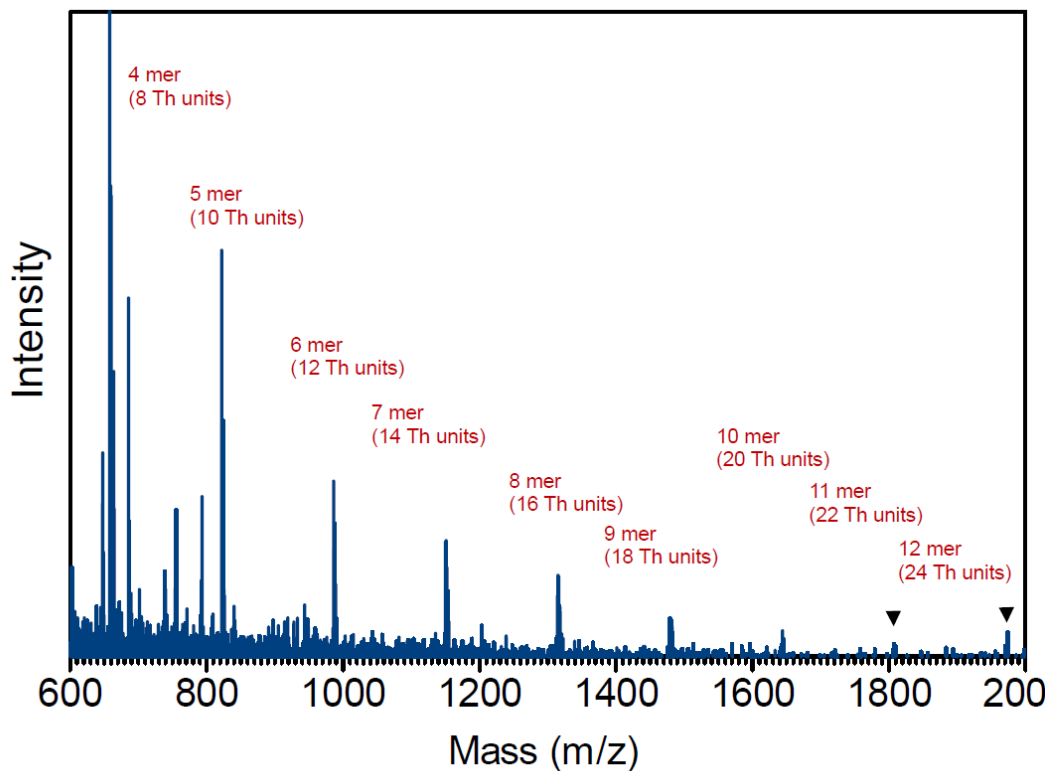


Figure S11. Matrix assisted laser desorption ionization, time of flight-mass (MALDI TOFF-MS) result of the polymer prepared in cholesteric liquid crystal electrolyte solution.

MOLECULAR WEIGHTS

Ionization of high molecular weight fractions may not be performed completely in the TOFF-MASS. Also, high molecular weight molecules tend to decrease arrival probability at the detector of the TOFF-MASS. Therefore, the signal intensity is not always proportional to amounts of the molecular weights of each fraction of the polymers.

The molecular weights obtained from the TOFF-MASS measurements may be reference indexes. In the present study the MALDI TOFF-MASS results may indicate that M_n , M_w , and dispersity are to be 806 g/mol, 913 g/mol, and 1.13, respectively with an assumption of the signal intensity was proportional to number of the molecules, although only the low molecular weight parts of the polymer can be estimated by the present TOFF-MASS spectroscopy measurements. The TOFF-MASS measurements exactly indicate sequence of the molecular repeat units of the polymer.

PLAUSIBLE REFLECTION MECHANISM

Exoskeleton of beetles with cholesteric-nematic-cholesteric order reflects circular polarized light by using multilayer structure. The multilayer polymer film thus prepared in this study is comparable to reflection functionality of the photonic insects.

The multilayer polymer may have the same light reflection mechanism as natural photonic insects with LC order (Caveney, S, *Proc. R. Soc. London*, 1971, Ser. **B178**, 205–225). Plausible mechanism of the reflection is described as follows.

Firstly, the top layer of the film with cholesteric order may reflect right-handed circular polarized light (R-CPL), and left-handed circular polarized light (L-CPL) passes through the top layer with incidence of natural non polarized light (R-CPL + L-CPL light). Subsequently, the middle layer with nematic order converts L-CPL into R-CPL. Finally, bottom cholesteric ordered layer reflects R-CPL (Figure S11). Therefore, the CD shows negative signals (right-handed polarized direction), as a result of gain loss of R-CPL due to reflection at low voltage (dedoped state). The gain loss due to reflection and absorption result in the CD signals. In the doped state, helicity of the cholesteric ordered layer is changed, and R-CPL can be reflected from the polymer. This may not be perfect for the PBT(Ch*-N-Ch*) having fingerprint pattern (homogeneous structure, helical axis is parallel to the layer) because this process is effective for Grandjean cholesteric LC alignment (planar structure, helical axis is perpendicular direction to the substrate).

The multilayer polymer thus prepared in this study can reflect R-CPL, and L-CPL passes through the film. Simultaneously, optical absorption is carried out. Optical

rotation of the polymer occurs for left direction (positive values in the ORD), as shown in Figure 7(c). The reflections are based on Ch*-N-Ch* order. However, the incompleteness of the light reflection functionality of the triple layer may pass residual light as an output. The trough of the CD corresponds to peak top of the ORD signal in this case, although a maximum in the ORD corresponds to inflection point of the CD in general. The CD and ORD signals do not always correspond to the optical absorption in the multilayer polymer. Furthermore, optical absorption of the polymer decreases a certain wavelength range of reflection light.

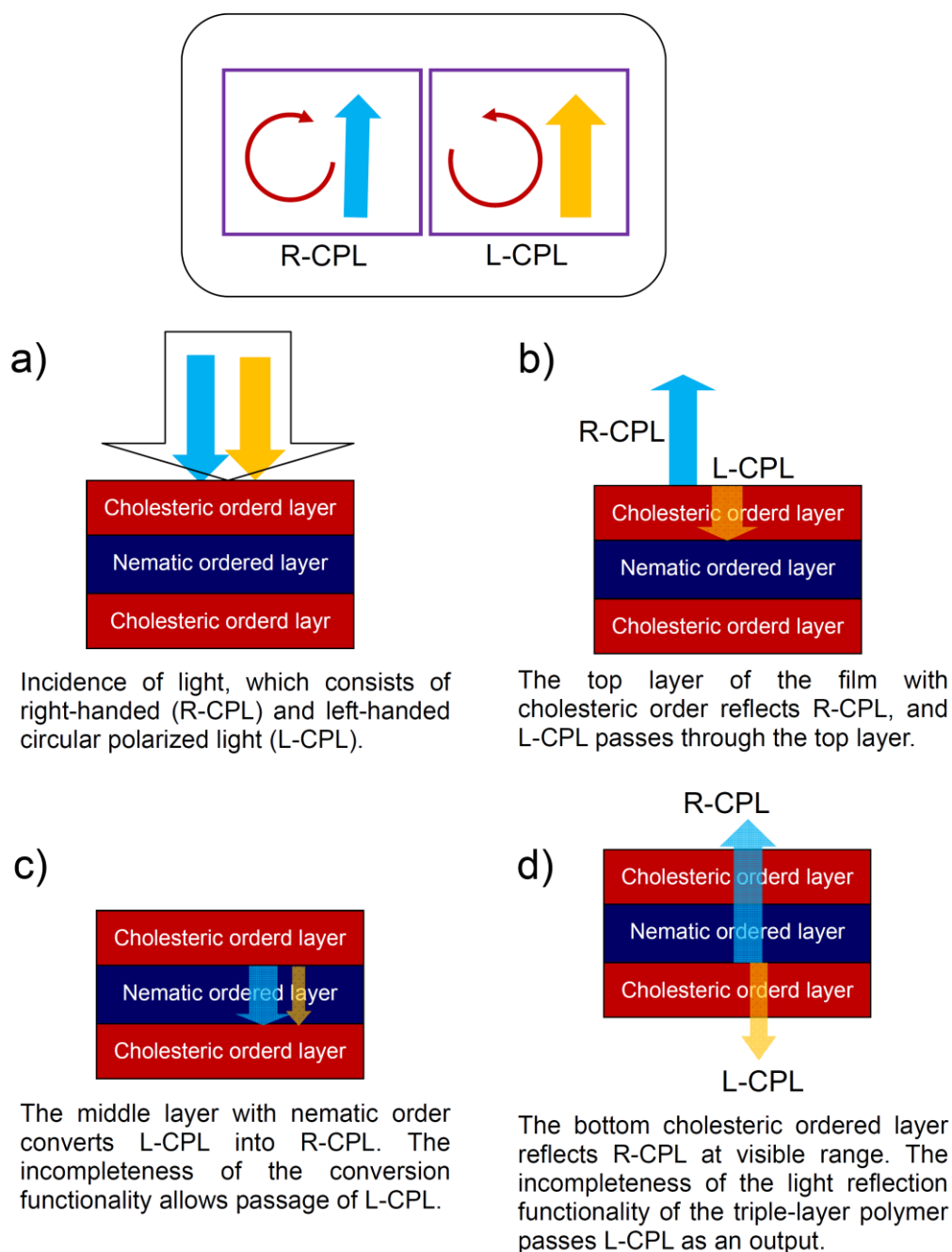


Figure S12. Possible model of light reflection function of the triple-layer polymer having cholesteric-nematic-cholesteric order with light passage process from (a) to (d).